

## EFFECT OF HEAT SOURCE/SINK ON MHD SLIP FLOW IN A CONVECTIVELY HEATED POROUS VERTICAL CHANNEL

M.Z. Shehu<sup>1</sup>, A. Umar<sup>2</sup> and M. Umar<sup>3</sup>

<sup>1,2,3</sup>Department of Mathematics Sokoto State University  
Sokoto, Nigeria.

[mzayyad015@gmail.com](mailto:mzayyad015@gmail.com)

08039369264

Corresponding author: M.Z. Shehu

### ABSTRACT

An adventure to trace the effect of heat source/sink on MHD slip flow in a convectively heated porous vertical channel is achieved. The analytical solution of the set of differential equation is derived by perturbation method. The influence of some active parameters such as Hartman number( $Ha$ ), Navier slip parameter( $\lambda$ ), Frank-Kamenetskii parameter( $\lambda$ ), Suction/injection parameter( $S$ ) and heat source/sink parameter( $Q$ ) are discussed on velocity, temperature, skin friction and Nusselt Number in details and line graph. The results show that; Velocity, Temperature together with Skin friction and Nusselt number (at  $y=0$ ) decrease with a rise in Heat Source/sink parameter( $Q$ ) but the skin friction and Nusselt number rise at  $y=l$

### 1.0 INTRODUCTION

The study on the effect of heat source/sink continue to inspire researchers in different field owing to its application in industries. In a fluid transportation, heat source and sink play a role where as heat source increase its thermal conductivity which increases the fluid temperature consequently. Where as the heat sink on the other side decreases the thermal conductivity which decreases the fluid temperature. Bhattacharyya [1] discussed the combine effect of heat source/sink, suction/injection and radiation on boundary layer past a shrinking surface, in which he concluded that the thermal boundary layer thickness has a decreasing chance with Prandtl number, heat sink and radiation parameter variation but enhanced with heat source. The analysis

of important of heat source/sink in natural convective flow was analyzed by Kumar and Singh [2], where the study indicated that the velocity increased with heat source but opposite in heat sink. Alsabery *et.al* [3] investigate the role of heat source/sink in free convective flow in a cylindrical cavity, which show that volume fraction augment of nanoparticles increases heat transfer. The numerical analysis of the role of thermal and hydraulic behaviour of micro latticed pin fin in the heat sink was analyzed by Wang *et.al* [4], where the researcher show that the latticed pin fin decreases the intensity of heat sink when considering the weight lost.

The effect of heat source/sink on MHD refers to how the addition or subtraction of heat influence the behavior of electrically conducting fluids, such as plasma or liquid metals in present of magnetic field, such as temperature distribution where the heat source introduces additional thermal energy into the system, which rise the temperature of the fluid while the heat sink removes the energy which causes cooling of the temperature. Density variation which changing in temperature result to variations in fluid density. More so, the heat source/sink in MHD system affect magnetic field behaviors, MHD equations, thermoelectric effects e.t.c. The important of heat source/sink on MHD nanofluid using homotopy analysis was discussed by Tlau and Ontela [5] where the result shows that both the skin friction and rate of heat transfer is higher in heat source compare to heat absorption. The effect of heat source on MHD start up natural convective flow in an annulus with isothermal and isoflux boundaries was analyzed by Yusuf *et.al* [6]. Kumar *et.al* [7] discussed the influence of heat source/sink on MHD flow between vertical alternate conducting walls with hall effect. Sharma and Singh [8] analyzed the influence of variable thermal conductivity and heat source/sink on MHD flow near a stagnation point in a linear stretching sheet. The effect of heat source/sink on MHD flow and heat transfer over a shrinking sheet with mass suction was investigated by Bhattacharyya [9]. Babu *et.al* [10] have studied the effects of radiation and heat source/sink on the steady state two dimensional MHD boundary layer flow past a shrinking sheet with wall mass suction by numerical techniques.

Slip flow has several practical applications in various field such as microfluidics where channels have dimensions on the order of micrometers, slip flow effects can be significant. Understanding slip flow is crucial for designing and optimizing these devices, used in areas like lab-on-a-chip technology and medical diagnostics. Gas transport, slip flow is relevant in gas transport through microscale and nanoscale channels which can affect the performance of gas sensors, gas separation membranes and devices used in the semi-conductor industry. Other application of slip flow include; Heat transfer, Aerospace engineering, vacuum technology, nanotechnology and

environmental monitoring. MHD slip flow and convective heat transfer due to a moving plate with effects of variable viscosity and thermal conductivity was analyzed by Nandeppanavar *et.al* [11]. Hamza [12] studied free convection slip flow of an exothermic fluid in a convectively heated vertical channel. Many applications on MHD slip flow has been conducted by such as Hamza *et.al* [13], Hamza *et.al* [14], Muhammad Zayyad Shehu *et.al* [15]. The present research will investigate the effect of heat source/sink on MHD slip flow in a convectively heated porous vertical channels.

## 2.0 MATHEMATICAL ANALYSIS

Looking at a time dependent natural convection flow of electrically conducting fluid in a vertical channels formed by two infinite vertical parallel plates separated by a distance H as shown in fig. with navier slip and newthonian heating. Following Hamza *et.al* [14] and Muhammad Zayyad Shehu *et.al* [15].

The non-dimensional governing equations under the Boussinesq's approximation can be written as;

$$v \frac{d^2 u'}{dy'^2} + v_0 \frac{du'}{dy'} + g\beta(T' - T'_0) - \frac{\nabla B_0^2 u'}{\rho} = 0 \quad (1)$$

$$\frac{k}{\rho c_p} \frac{d^2 T'}{dy'^2} + v_0 \frac{dT'}{dy'} + \frac{QC_0^* A}{\rho c_p} e^{\left(\frac{-E}{RT'}\right)} + \frac{Q_0}{\rho c_p} = 0 \quad (2)$$

The boundary conditions for the present problem are

$$\left. \begin{aligned} u' &= \gamma^* \frac{du'}{dy'}, -k \frac{dT'}{dy'} = h[T'_0 - T'], \text{ at } y' = 0 \\ u' &= 0, T' = T'_0 \text{ at } y' = H \end{aligned} \right\} \quad (3)$$

where  $\beta$  is the coefficient of thermal expansion,  $Q$  is the heat of reaction,  $A$  is the rate constant,  $E$  is the activation energy,  $R$  is the universal constant,  $\nu$  is the kinematic viscosity,  $C_0$  is the initial concentration of the reactant species,  $g$  is the gravitational force,  $C_p$  is the specific heat at constant pressure and  $k$  is the thermal conductivity of the fluid, while  $\rho$  is the density of the fluid and  $Q_0$  is the heat source

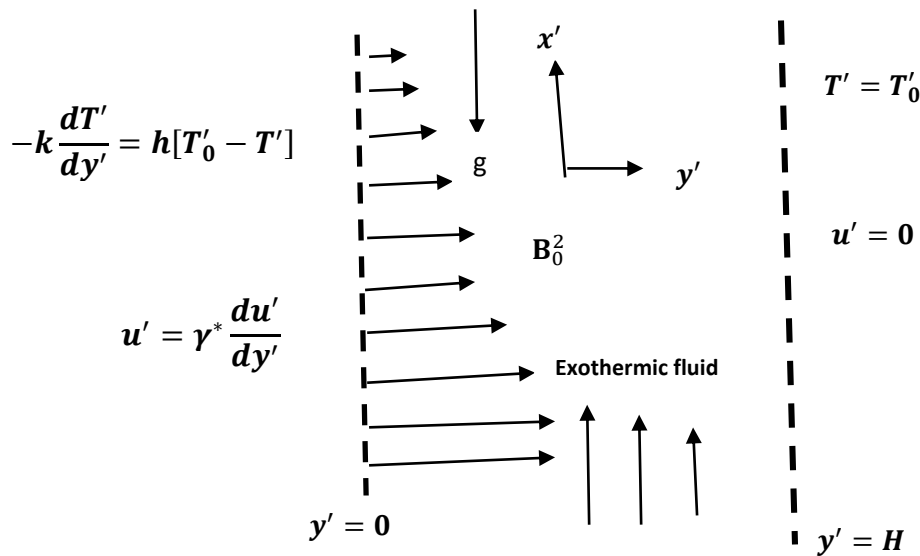


**Figure 1:** Geometry of the problem

To solve equations (1) and (2), we employ the following dimensionless variables and parameters

$$\left. \begin{aligned} y = \frac{y'}{H}, \theta = \frac{E(T' - T_0)}{RT_0^2}, \varepsilon = \frac{RT_0}{E}, U = \frac{u' \mu_0 E}{g \beta H^2 RT_0^2}, \lambda = \frac{QC_0^* AEH^2}{RT_0^2} e^{\left(\frac{-E}{RT_0}\right)}, Pr = \frac{\mu_0 \rho C_p}{k} \\ \gamma = \frac{\gamma^*}{H}, \theta_a = \frac{E(T_a - T_0)}{RT_0^2}, Br = \frac{hH}{k}, Q = \frac{Q_0}{k} \end{aligned} \right\} \quad (4)$$

Using (4), Equations (1)-(3) take the following form:

$$\frac{d^2 U}{dy^2} + S \frac{dU}{dy} - Ha^2 U = -\theta \quad (5)$$

$$\frac{d^2 \theta}{dy^2} + SPr \frac{d\theta}{dy} + \lambda e^{\left(\frac{\theta}{1+\varepsilon\theta}\right)} - Q\theta = 0 \quad (6)$$

$$\left. \begin{aligned} U - \gamma \frac{dU}{dy} = 0, \frac{d\theta}{dy} - Br[\theta - \theta_a] = 0 \text{ at } y = 0 \\ U = 0, \theta = 0, \text{ at } y = 1 \end{aligned} \right\} \quad (7)$$

Where  $Pr, \gamma, Br, \lambda, \theta_a, Ha, S, Q$  and  $\varepsilon$  are Prandtl number, Navier slip parameter, Biot number, Frank-Kamenetskii parameter, ambient temperature, Hartmann number, Suction/Injection parameter, Heat Source/Sink parameter and activation energy parameter.

### 3.0 METHOD OF SOLUTION

To obtain the approximate solutions, we take the power series expansion in Frank-Kamenetskii parameter  $\lambda$  of the form:

$$\left. \begin{aligned} U &= U_0 + \lambda U_1 + \lambda^2 U_2 + o(\lambda) \\ \theta &= \theta_0 + \lambda \theta_1 + \lambda^2 \theta_2 + o(\lambda) \end{aligned} \right\} \quad (8)$$

Substituting (8) into (5)-(7) and equating the coefficient of like powers of  $\lambda$ , the resulting solutions of the momentum and energy balance equations are as follows:

$$\begin{aligned} U &= B_{31}e^{m_1y} + B_{32}e^{-m_2y} + C_{31} + C_{32}e^{-ky} \\ &+ \lambda[B_{33}e^{m_1y} + B_{34}e^{-m_2y} + v_{30} + v_{31}y + v_{32}e^{-ky} + v_{33}ye^{-ky} + v_{34}e^{-2ky} \\ &+ v_{35}e^{-3ky}] \\ &+ \lambda^2[B_{35}e^{m_1y} + B_{36}e^{-m_2y} + h_0 + h_1y + h_2y^2 + h_3e^{-ky} + h_4ye^{-ky} + h_5y^2e^{-ky} \\ &+ h_6e^{-2ky} + h_7ye^{-2ky} + h_8e^{-3ky}] \end{aligned} \quad (9)$$

$$\begin{aligned} \theta &= A_{31} + A_{32}e^{-ky} + \lambda[A_{33} + A_{34}e^{-ky} + s_{30}y + s_{31}ye^{-ky} + s_{32}e^{-2ky} + s_{33}e^{-3ky}] \\ &+ \lambda^2[A_{35} + A_{36}e^{-ky} + t_{30}y + t_{31}y^2 + t_{32}ye^{-ky} + t_{33}y^2e^{-ky} + t_{34}e^{-2ky} \\ &+ t_{35}ye^{-2ky} + t_{36}e^{-3ky}] \end{aligned} \quad (10)$$

From (9), the steady state skin frictions on the boundaries are as follows:

$$\begin{aligned} \frac{dU}{dy} \Big|_{y=0} &= m_1B_{31} - m_2B_{32} - kC_{32} \\ &+ \lambda[m_1B_{33} - m_2B_{34} + v_{31} - kv_{32} + v_{33} - 2kv_{34} - 3kv_{35}] \\ &+ \lambda^2[m_1B_{35} - m_2B_{36} + h_1 - kh_3 + h_4 - 2kh_6 + h_7 - 3kh_8] \end{aligned} \quad (11)$$

$$\begin{aligned} \frac{dU}{dy} \Big|_{y=1} = & m1B_{31}e^{m1} - m2B_{32}e^{-m2} - kC_{32}e^{-k} \\ & + \lambda[m1B_{33}e^{m1} - m2B_{34}e^{-m2} + v_{31} - kv_{32}e^{-k} + v_{33}[e^{-k} - ke^{-k}] \\ & - 2kv_{34}e^{-2k} - 3kv_{35}e^{-3k}] \\ & + \lambda^2[m1B_{35}e^{m1} - m2B_{36}e^{-m2} + h_1 + 2h_2 - kh_3e^{-k} + h_4[e^{-k} - ke^{-k}] \\ & + h_5[2e^{-k} - ke^{-k}] - 2kh_6e^{-2k} + h_7[e^{-2k} - 2ke^{-2k}] - 3kh_8e^{-3k}] \end{aligned} \quad (12)$$

Also, from (10) the rates of heat transfer on the boundaries in terms of Nusselt number are as follows:

$$\begin{aligned} \frac{d\theta}{dy} \Big|_{y=0} = & -kA_{32} + \lambda[-kA_{34} + s_{30} + s_{31} - 2ks_{32} - 3ks_{33}] \\ & + \lambda^2[-kA_{36} + t_{30} + t_{32} - 2kt_{34} + t_{35} - 3kt_{36}] \end{aligned} \quad (13)$$

$$\begin{aligned} \frac{d\theta}{dy} \Big|_{y=1} = & -A_{32}e^{-k} + \lambda[-kA_{34}e^{-k} + s_{30} + s_{31}[e^{-k} - ke^{-k}] - 2ks_{32}e^{-2k} - 3ks_{33}e^{-3k}] \\ & + \lambda^2[-kA_{36}e^{-k} + t_{30} + 2t_{31} + t_{32}[e^{-k} - ke^{-k}] + t_{33}[2e^{-k} - ke^{-k}] - 2kt_{34}e^{-2k} \\ & + t_{35}[e^{-2k} - 2ke^{-2k}] - 3kt_{36}e^{-3k}] \end{aligned} \quad (14)$$

#### 4.0 RESULT AND DISCUSSION

The basic parameters that govern this flow are Magnetic field parameter (Ha), Navier slip parameter( $\gamma$ ), Biot number(Br), Frank-Kamenetskii parameter( $\lambda$ ), Suction/injection parameter(S) and Heat source/sink parameter(Q). Unless stated otherwise, the following parameters remain unchanged,  $Pr=0.71$ ,  $\varepsilon=0.01$ ,  $\theta_a = 1$ . The effects of those parameters have been analyzed with the aid of line graph indicated in Fig. (4.3.1) to (4.3.4).

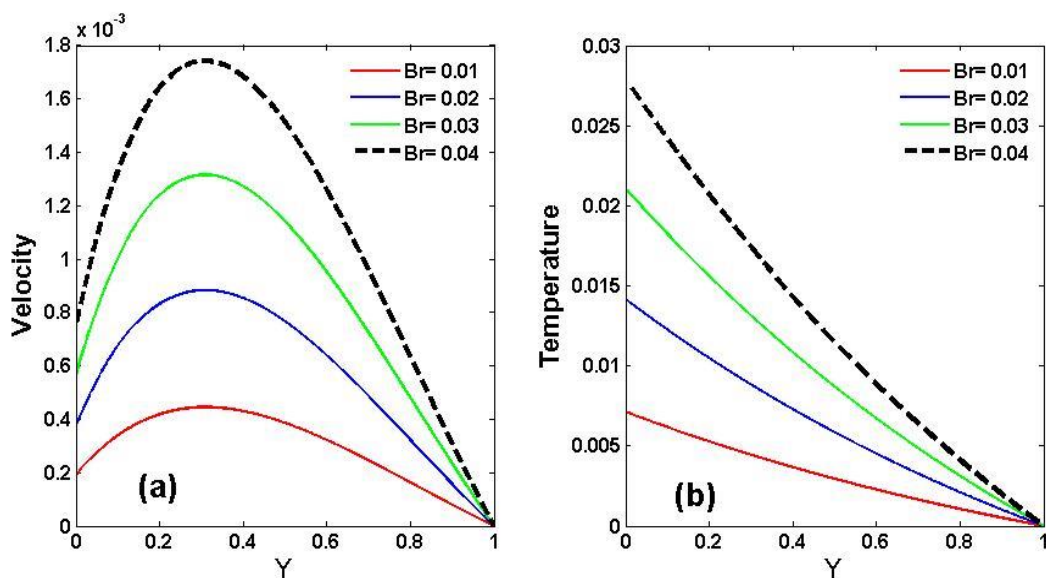


Figure 2: Effect of Biot number ( $Br$ ) on Velocity and Temperature with  $Ha=1$ ,  $S=1$ ,  $\gamma=0.1$ ,  $\lambda=0.1$ ,  $S=1$ ,  $Q=0.1$

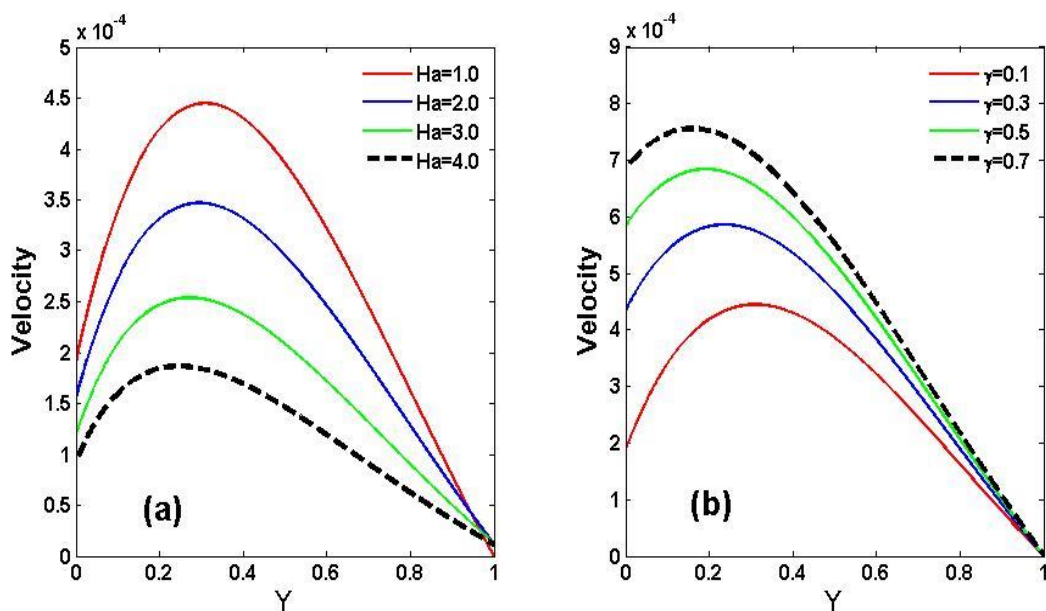


Figure 3: Effect of Hartmann number ( $Ha$ ) and Navier slip parameter ( $\gamma$ ) on Velocity with  $Br=0.01$ ,  $\lambda=0.01$ ,  $S=1$ ,  $Q=0.1$  and  $\gamma=0.1$  in fig. (a) and  $Ha=5$  in fig. (b).

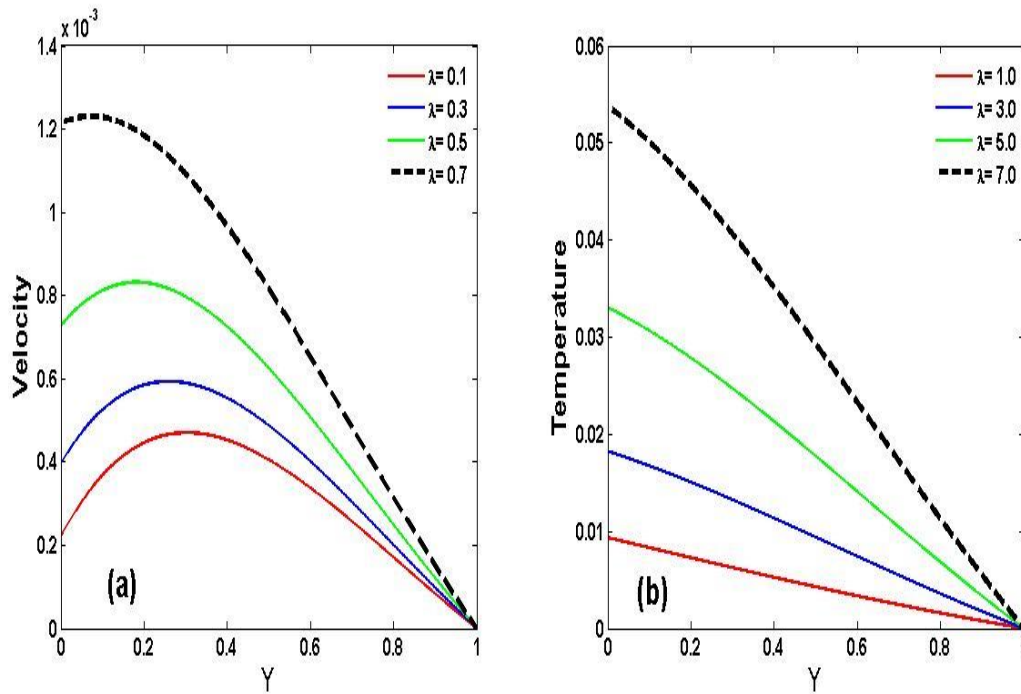


Figure 4: Effect of Frank-Kamenetskii parameter ( $\lambda$ ) on Velocity and Temperature with  $Ha=1, \gamma=0.1, S=1, Q=0.1, Br=0.01$

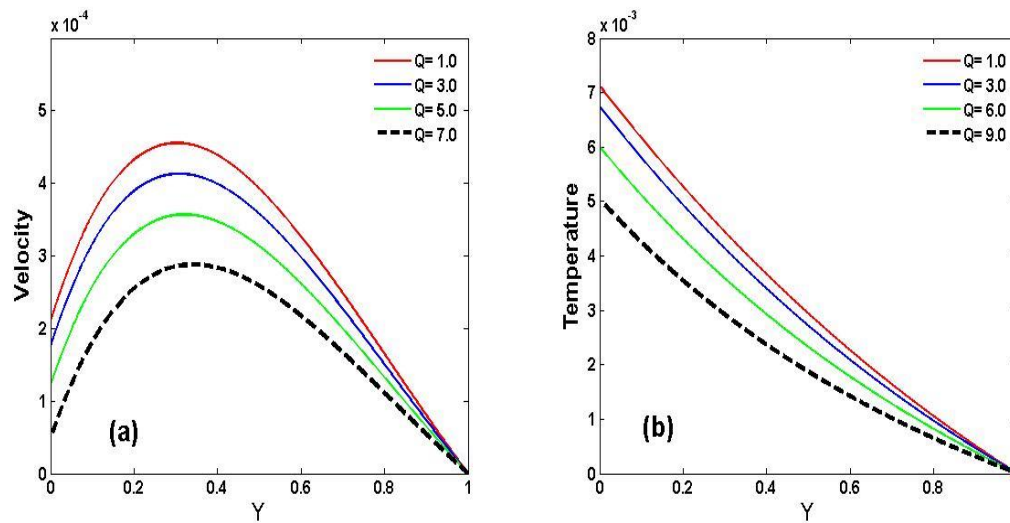


Figure 5: Effect of Heat source/sink parameter on Velocity and Temperature with  $Ha=1, \gamma=0.1, \lambda=0.1, S=1, Br=0.01$



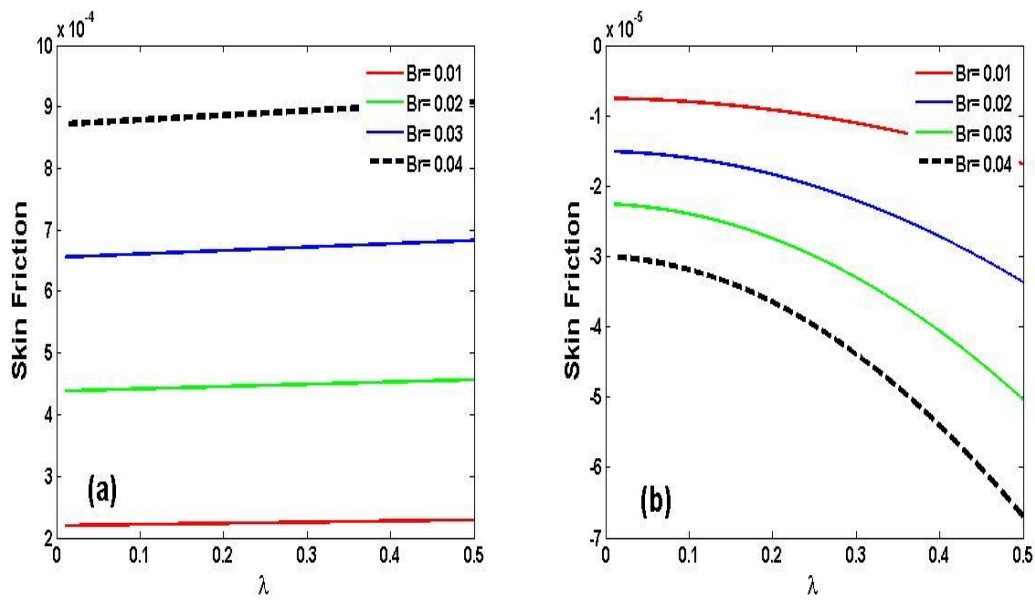


Figure 6: Effect of Biot number (Br) on Skin friction for distance  $y=0$  and  $y=1$  with  $Ha=5, \gamma=0.1, \lambda=0.01, S=5, Q=0.1$

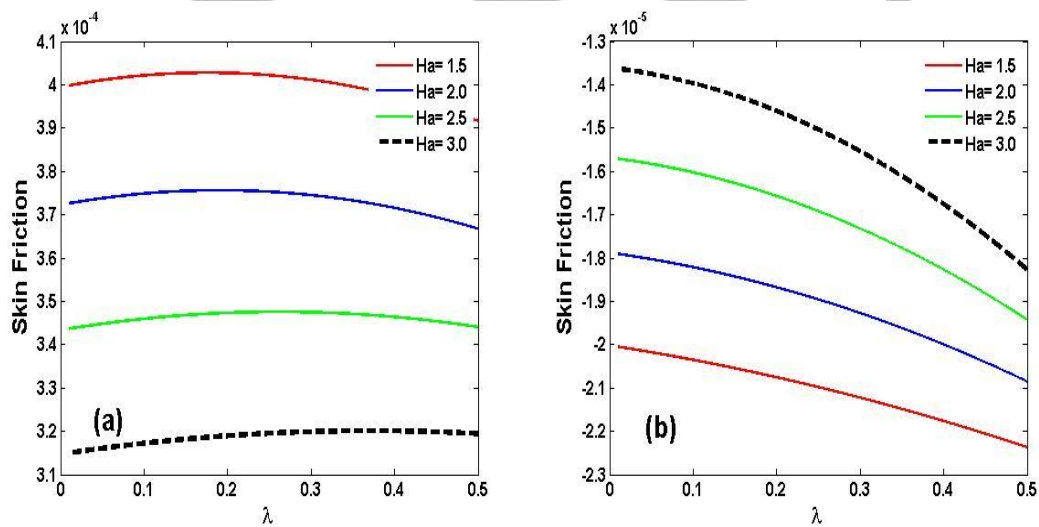


Figure 7: Effect of Hartmann number (Ha) on Skin friction for distance  $y=0$  and  $y=1$  with  $Br=0.01, \gamma=0.1, \lambda=0.01, S=5, Q=0.1$

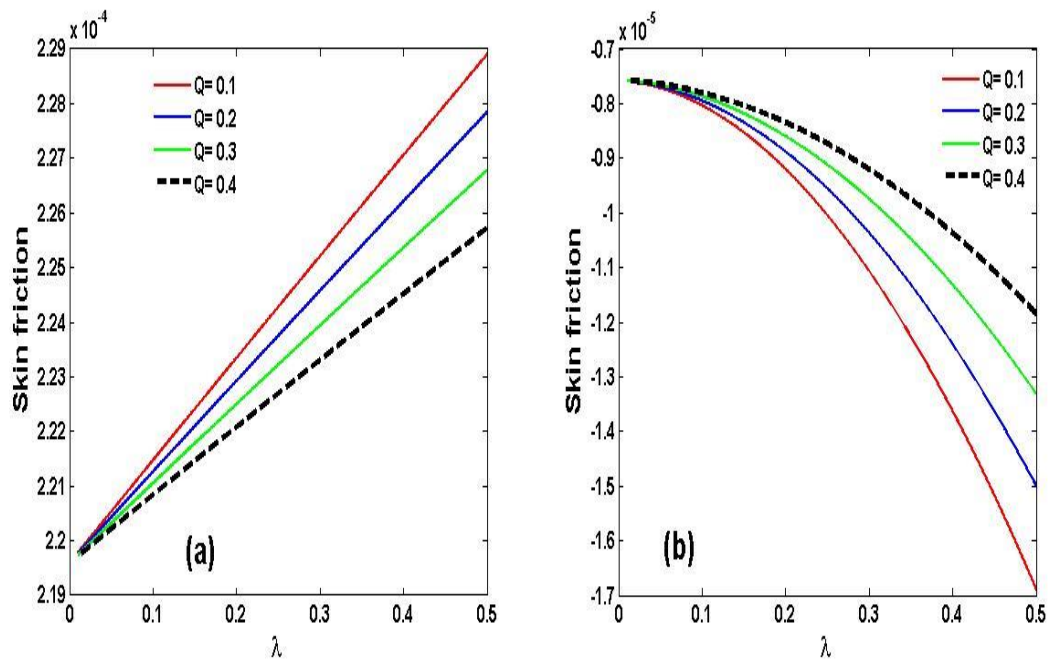


Figure 8: Effect of Heat source/sink parameter ( $Q$ ) on Skin friction at distance  $y=0$  and  $y=1$  with  $Ha=5$ ,  $\gamma=0.1$ ,  $\lambda=0.01$ ,  $S=5$ ,  $Br=0.01$

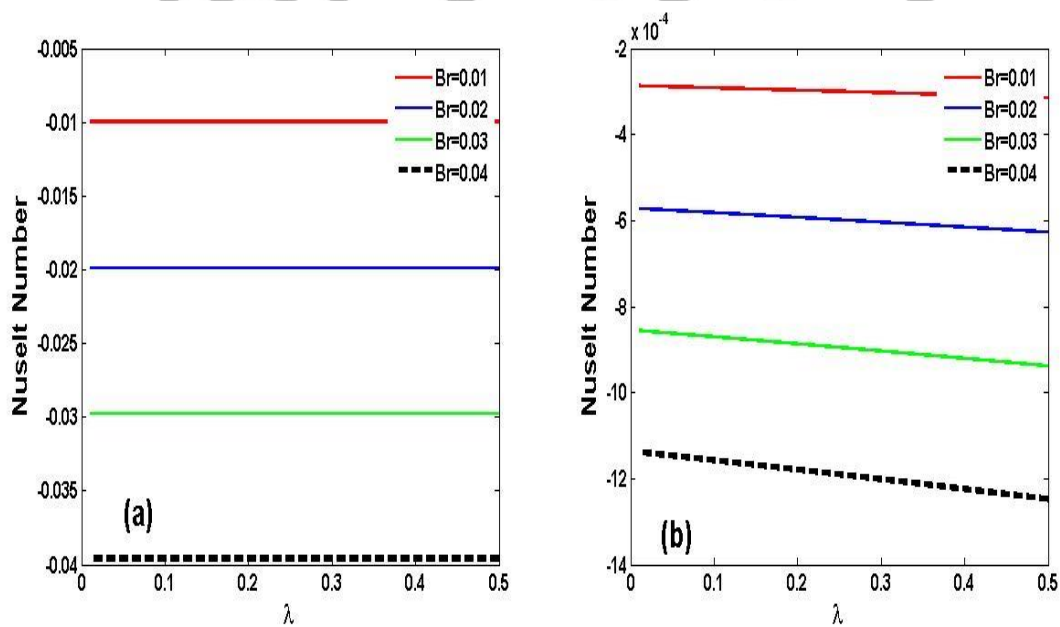


Figure 9: Effect of Biot number ( $Br$ ) on Nusselt number on a distance  $y=0$  and  $y=1$  with  $Ha=5$ ,  $\gamma=0.1$ ,  $\lambda=0.1$ ,  $S=5$ ,  $Q=0.1$

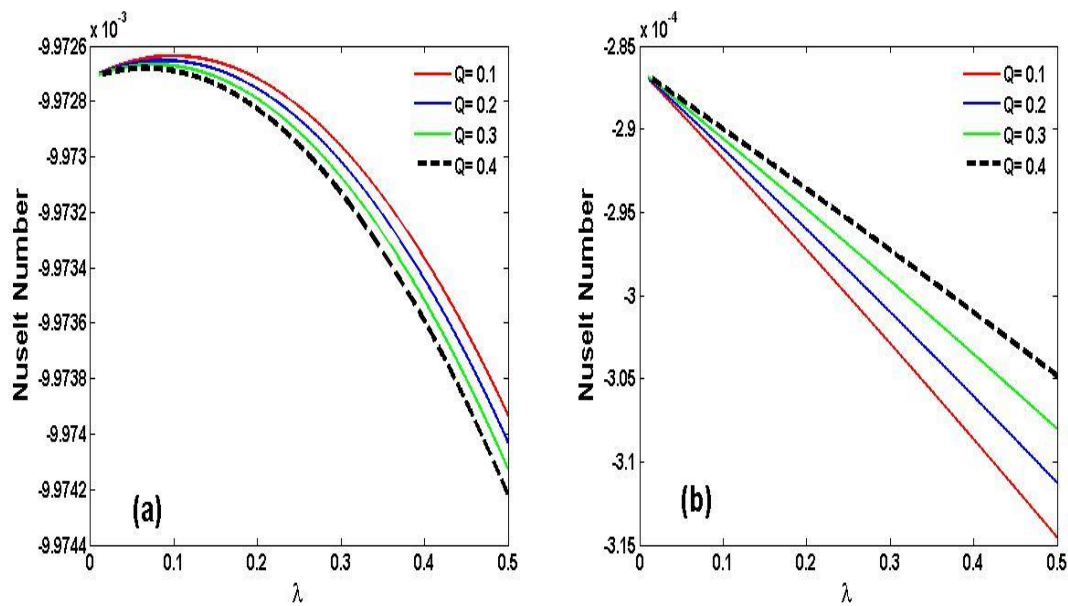


Figure 10: Effect of Heat source/sink parameter on Nusselt number on a distance  $y=0$  and  $y=1$  with  $Ha=5$ ,  $\gamma=0.1$ ,  $\lambda=0.1$ ,  $S=5$ ,  $Q=0.1$

Influence of Biot number ( $Br$ ) on velocity and temperature are shown in figure 2a and figure 2b respectively, where increase in  $Br$ , increases the velocity and temperature profile. Hartmann number ( $Ha$ ) and Navier slip parameter( $\gamma$ ) effect are shown in figure 3, where figure 3a show that increase in  $Ha$  lead to decrease in velocity, but increase in  $\gamma$ , increases the velocity profile as seen in figure 3b. An increase in Frank-Kamenetskii parameter ( $\lambda$ ) lead to an increase in velocity profile as shown in figure 4a and also increase in Frank Kamenetskii parameter  $\lambda$ , increases the temperature profile, see figure 4b. Lastly, we have seen the effect of heat generating and absorbing parameter ( $Q$ ) on velocity and temperature, as both the velocity and temperature profile decreases with an increase in  $Q$ , see figure 5a and figure 5b respectively.

Skin friction increases with an increase in Biot number ( $Br$ ) on distance  $y=0$  but decrease with an increase in  $Br$  for distance  $y=1$ . See figure 6a and b respectively. Increase in Hartmann number lead to decrease in skin friction for  $y=0$  and increases for  $y=1$ . See figure 7a and b respectively.

Skin friction decreases with an increase in heat source/sink parameter ( $Q$ ) for  $y=0$  but it increases skin friction for  $y=1$  as shown in figure 8a and b respectively. The effect of Biot number ( $Br$ ) on Nusselt number is shown in figure 9a and b, as increase in  $Br$ , decreases the Nusselt number for both  $y=0$  and  $y=1$ . Heat generating/absorbing fluid has effect on Nusselt number, as it decreases the rate of heat transfer with an increase in  $Q$  at  $y=0$  but increases rate of heat transfer at  $y=1$ . See figure 10a and b respectively.

## 5.0 CONCLUSION

The present paper analyze the effect of heat source/sink on MHD slip flow in a convectively heated porous vertical channel. The analytical solution of the problems where solve using perturbation method. The summary of the major finding are as follows;

1. An increase in  $Ha$  result to a slippage in velocity and skin friction at  $y=0$  but the skin friction rises at  $y=1$
2. The rise in  $Q$  lead to a decrease in velocity, temperature and also skin friction with Nusselt number at  $y=0$ , but that changes the flow of skin friction and Nusselt number to rise at  $y=1$
3. Both velocity, temperature and skin friction (at  $y=0$ ) rises with increase in biot number ( $Br$ ) but at  $y=1$ , the skin friction decline.
4. An increase in Frank kamenetskii parameter ( $\lambda$ ) rise the flow of both velocity and temperature

## REFERENCES

1. Lavanya B., & Ratnam A.L. (2014). Radiation and mass transfer effects on unsteady MHD free convection flow pasta vertical porous plate embended in a porous medium in a slip flow regime with heat source/sink and solet effect. *Int. J Eng Tech Res.* 2(11), 210-220
2. Kumar D., & Singh A.K. (2016). Effect of heat source/sink and induced magnetic field on natural convective flow in vertical concentric annuli. *Alexandria Eng J.* 55(4), 3125-3133

3. Alsabery A.L., Gedik E., Chamkha A.J., & Hashim I. (2019). Effect of two-phase nanofluid model and localized heat source/sink on natural convection in a square cavity with a solid circular cylinder. *Comput Methods Appl Mech Eng.* 346, 952-981
4. Wang X., Chen M., Tate D., Rahimi H., & Zhang S. (2020). Numerical investigation on hydraulic and thermal characteristics of micro latticed pin fin in the heat sink. *Int J Heat Mass Transf.* 149, 119157
5. Tlau L., & Ontela S. (2019). Entropy generation in MHD nanofluid flow with heat source/sink. *SN Appl Sci.* 1(12), 1672
6. Yusuf S.T., Dauda G., & Adebayo H.O. (2020). Effect of heat source/sink on MHD startup natural convective flow in an annulus with isothermal and isoflux boundaries. *Arab Journal of Basic and Applied Science.* 27(1), 365-374
7. Kumar D., Singh A.K., & Kumar D. (2020). Influence of heat source/sink on MHD flow between alternate conducting walls with hall effect. *Physica A: Statistical Mechanics and its Applications.* 544, 123562.
8. Sharma P.R., & Singh G. (2009). Effect of variable thermal conductivity and heat source/sink in MHD flow near a stagnation point on a linearly stretching sheet. *J.Appl. fluid Mech.* 2(1), 13-21
9. Bhattacharyya K. (2011). Effect of radiation and heat source/sink on unsteady MHD boundary layer flow and heat transfer over a shrinking sheet with suction/injection. *Front. Chem. Sci. Eng.* 5(3), 376-384
10. Babu P.R., Rao J.A. Sheri S. (2014). Radiation Effect on MHD heat and mass transfer flow over a shrinking sheet with mass suction. *J. Appl. Fluid. Mech.* 7(4), 641-650
11. Nandeppanavar, M.M., Kemparaju M.C., Madhusudhan R & Vaishali S. (2020). MHD slip flow and convective heat transfer due to a moving plate with effect of variable viscosity and thermal conductivity. *Multidiscipline Modelling in Materials and Structures.* 16(5), 991-1018
12. Hamza M.M.(2016). Free convection slip flow of an exothermic fluid in a convectively heated vertical channel. *Ain Shams Engineering Journal.* 9(4), 1313-1323
13. Hamza M.M, Shehu M.Z. and Tambuwal B.H (2021). Steady State MHD free convectional slip flow of an exothermic fluid in a convectively heated vertical channel. *Saudi J. Eng. Technol.* 6(10), 364-370.
14. Hamza M.M, Shehu M.Z., Usman H. and Omokhuale E.(2022). Computational Treatment of Transient MHD slip flow of an Arrhenius Chemical reaction in a convectively heated vertical channel. *CaJoST.* 2, 231-237
15. Shehu M.Z, Abdullahi I., Umar M (2022). MHD slip flow of an exothermic fluid in a convectively heated porous vertical channel. *Saudi J. Eng. Technol.* 7(10), 542-549

## APPENDIX

$$k = SPr$$

$$A_{32} = \frac{-Br\theta_a}{Br(e^{-k}-1)-k}, A_{31} = -A_{32}e^{-k}$$

$$r_0 = (Q - 1)A_{31} + \varepsilon A_{31}^2 \left(1 - \frac{\varepsilon A_{31}}{2}\right), r_1 = (Q - 1)A_{32} + \varepsilon A_{31} A_{32} \left(2 - \frac{3\varepsilon A_{31}}{2}\right), r_2 = \varepsilon A_{32}^2 \left(1 - \frac{3\varepsilon A_{31}}{2}\right),$$

$$r_3 = \frac{-\varepsilon^2 A_{32}^3}{2}, s_0 = \frac{r_0}{k}, s_1 = \frac{r_1}{-k}, s_2 = \frac{r_2}{2k^2}, s_3 = \frac{r_3}{6k^2}, w_1 = -k - Br, w_2 = -2k - Br, w_3 = -3k - Br$$

$$A_{34} = \frac{[s_{30}(1+Br)+s_{31}(1+Bre^{-k})-s_{32}(w1-Br e^{-2k})-s_{33}(w2-Br e^{-3k})]}{k+Br-Br e^{-k}},$$

$$A_{33} = -[A_{34}e^{-k} + s_{30} + s_{31}e^{-k} + s_{32}e^{-2k} + s_{33}e^{-3k}],$$

$$n_0 = 2\varepsilon(A_{31}A_{33}) + A_{33}(Q - 1) - \frac{3\varepsilon^2 A_{31}^2 A_{33}}{2},$$

$$n_1 = 2\varepsilon(A_{31}s_{30}) + s_{30}(Q - 1) - \frac{3\varepsilon^2 A_{31}^2 s_{30}}{2}$$

$$n_2 = 2\varepsilon(A_{31}s_{31} + A_{32}A_{33}) + A_{34}(Q - 1) - \frac{3\varepsilon^2(A_{31}^2 A_{34} + 2A_{31}A_{32}A_{33})}{2},$$

$$n_3 = 2\varepsilon(A_{31}s_{32} + A_{32}s_{30}) + s_{31}(Q - 1) - \frac{3\varepsilon^2(A_{31}^2 s_{31} + 2A_{31}A_{32}s_{30})}{2},$$

$$n_4 = 2\varepsilon(A_{31}s_{32} + A_{32}A_{34}) + s_{32}(Q - 1) - \frac{3(2A_{31}A_{32}A_{34} + A_{31}^2 s_{32} + A_{32}^2 A_{33})}{2},$$

$$n_5 = 2\varepsilon(A_{32}s_{31}) - \frac{3\varepsilon^2(A_{32}^2 s_{30} + 2A_{31}A_{32}s_{31})}{2}.$$

$$n_6 = 2\varepsilon(A_{31}s_{33} + A_{32}s_{32}) + s_{33}(Q - 1) - \frac{3\varepsilon^2(A_{31}^2 s_{33} + 2A_{31}A_{32}s_{32} + A_{32}^2 A_{34})}{2},$$

$$t_{36} = \frac{n_6}{6k^2}, t_{35} = \frac{n_5}{2k^2}, t_{34} = \frac{n_4 + 3kt_5}{2k^2}, t_{33} = \frac{-n_3}{2k}, t_{32} = \frac{2t_{33} - n_2}{k}, t_{31} = \frac{n_1}{2k}, t_{30} = \frac{(n_0 - 2t_{31})}{k},$$

$$A_{36} = \frac{t_{36}(3k+Br-Br e^{-3k})+t_{34}(2k+Br-Br e^{-2k})-t_{35}(1-Br+Br e^{-2k})-t_{30}(1+Br)-t_{32}(1+Br e^{-k})-Br(t_{31}+t_{33}e^{-k})}{-k-Br-Br e^{-k}},$$

$$A_{35} = -[A_{36}e^{-k} + t_{30} + t_{31} + t_{32}e^{-k} + t_{33}e^{-k} + t_{34}e^{-2k} + t_{35}e^{-2k} + t_{36}e^{-3k}],$$

$$m1 = \frac{-S + \sqrt{S^2 + 4Ha^2}}{2}, m2 = \frac{-(S + \sqrt{S^2 + 4Ha^2})}{2}$$

$$c_{31} = \frac{A_{31}}{Ha^2}, c_{32} = \frac{-A_2}{k(k-S)-Ha^2},$$

$$B_{32} = \frac{c_{31}[(1-\gamma m1)e^{-m1}-1]+c_{32}[(1-\gamma m1)e^{-(m1+k)}]-(\gamma k+1)}{(1+\gamma m2)+(\gamma m1-1)e^{-(m1+m2)}},$$

$$B_{31} = -[B_{32}e^{-m2} + c_{31} + c_{32}e^{-k}]e^{-m1},$$

$$v_{35} = \frac{-s_{33}}{9k^2-3Sk-Ha^2}, v_{34} = \frac{-s_{32}}{4k^2-2Sk-Ha^2}, v_{33} = \frac{-s_{31}}{k^2-Sk-Ha^2}, v_{32} = \frac{v_{33}(2k-S)-A_{34}}{k^2-Sk-Ha^2},$$

$$v_{31} = \frac{s_{30}}{Ha^2}, v_{30} = \frac{A_{33}+Sv_{31}}{Ha^2},$$

$$w11 = (e^{m1+m2} + e^{m2}(\gamma m1 - 1)), w12 = (-\gamma e^{m1+m2} + e^{m2}(\gamma m1 - 1))$$

$$w13 = e^{m1+m2}(1 + \gamma k) + e^{m2}(\gamma m1 - 1), w14 = e^{m2-k}(\gamma m1 - 1),$$

$$w15 = e^{m1+m2}(1 + 2\gamma k) + e^{m2-2k}(\gamma m1 - 1), w16 = e^{m1+m2}(1 + 3\gamma k) + e^{m2-3k}(\gamma m1 - 1),$$

$$w17 = (1 - \gamma m1) - (1 + \gamma m2)e^{m1+m2}$$

$$B_{34} = \frac{v_{30}[e^{-m1}-1]+v_{31}[e^{-m1}+\gamma]+v_{32}[e^{-k-m1}-(\gamma k+1)]+v_{33}[e^{-k-m1}+\gamma]+v_{34}[e^{-2k-m1}-(2\gamma k+1)]+v_{35}[e^{-3k-m1}-(1+3\gamma k)]}{(1+\gamma m2)-e^{-m2-m1}}$$

$$B_{33} = -[B_{34}e^{-m2} + v_{30} + v_{31} + v_{32}e^{-k} + v_{33}e^{-k} + v_{34}e^{-2k} + v_{35}e^{-3k}]e^{-m1}$$

$$h_8 = \frac{-t_{36}}{9k^2-3Sk-Ha^2}, h_7 = \frac{-t_{35}}{4k^2-2Sk-Ha^2}, h_6 = \frac{-t_{34}+h_7(S-4k)}{4k^2-2Sk-Ha^2}$$

$$h_5 = \frac{-t_{33}}{k^2-Sk-Ha^2}, h_4 = \frac{-[t_{32}+h_5(2S-4k)]}{k^2-Sk-Ha^2}, h_3 = \frac{-[A_{36}+2h_5+h_4(S-2k)]}{k^2-Sk-Ha^2},$$

$$h_2 = \frac{t_{31}}{Ha^2}, h_1 = \frac{t_{30}+2Sh_2}{Ha^2}, h_0 = \frac{A_{35}+Sh_1+2h_2}{Ha^2}$$

$$w_{20} = e^{-m_1}(1 - \gamma m_1) + 1, w_{21} = e^{-m_1}(1 - \gamma m_1) - \gamma, w_{22} = (1 - \gamma m_1)e^{-m_1},$$

$$w_{23} = (1 + \gamma k) + (1 - \gamma m_1)e^{-m_1-k}, w_{24} = (1 - \gamma m_1)e^{-m_1-k} - \gamma, w_{25} = (1 - \gamma m_1)e^{-m_1-k},$$

$$w_{26} = (1 + 2\gamma k) + (1 - \gamma m_1)e^{-m_1-2k}, w_{27} = (1 - \gamma m_1)e^{-m_1-2k} - \gamma,$$

$$w_{28} = (1 + 3\gamma k) + (1 - \gamma m_1)e^{-m_1-3k},$$

$$B_{36} = \frac{[h_0w_{20}+h_1w_{21}+h_2w_{22}+h_3w_{23}+h_4w_{24}+h_5w_{25}+h_6w_{26}+h_7w_{27}+h_8w_{28}]}{(1+\gamma m_2)+(1-\gamma m_1)e^{-m_1-m_2}},$$

$$B_{35} = -[B_{36}e^{-m_2}+h_0 + h_1 + h_2 + (h_3 + h_4 + h_5)e^{-k} + (h_6 + h_7)e^{-2k} + h_8e^{-3k}]e^{-m_1},$$

